0013-7227/01/$03.00/0
Endocrinology

Vol. 142, No. 6
Printed in U.S.A.

Caspase-3 Gene Knockout Defines Cell Lineage Specificity for Programmed Cell Death Signaling in the Ovary*

TIINA MATIKAINEN†, GLORIA I. PEREZ, TIMOTHY S. ZHENG‡, THOMAS R. KLUZAK, BO R. RUEDA, RICHARD A. FLAVELL§, AND JONATHAN L. TILLY

Vincent Center for Reproductive Biology, Department of Obstetrics and Gynecology (T.M., G.I.P., B.R.R., J.L.T.), Massachusetts General Hospital/Harvard Medical School, Boston, Massachusetts 02114; Section of Immunobiology, Yale University School of Medicine (T.S.Z., R.A.F.), New Haven, Connecticut 06510; and Department of Obstetrics and Gynecology, University of Kansas School of Medicine, and Wesley Medical Center (T.R.K.), Wichita, Kansas 67214

ABSTRACT

Previous studies have proposed the involvement of caspase-3, a downstream executioner enzyme common to many paradigms of programmed cell death (PCD), in mediating the apoptosis of both germ and somatic cells in the ovary. Herein we used *caspase-3* gene knockout mice to directly test for the functional requirement of this protease in oocyte and/or granulosa cell demise. Using both *in vivo* and *in vitro* approaches, we determined that oocyte death initiated as a result of either developmental cues or pathological insults was unaffected by the absence of caspase-3. However, granulosa cells of degenerating antral follicles in both mouse and human ovaries showed a strong immunoreaction using an antibody raised against the cleaved (activated) form of caspase-3. Furthermore, *caspase-3* mutant female mice possessed aberrant atretic follicles containing granulosa cells that failed to be eliminated by apoptosis, as confirmed by TUNEL (terminal deoxynucleotidyl transferase-mediated deoxy-UTP nick end labeling) analysis of DNA cleavage and 4′,6-diamidino-2-phenylindole staining of nuclear morphology (pyknosis). These *in vivo* results were supported by findings from *in vitro* cultures of wild-type and caspase-3-deficient antral follicles or isolated granulosa cells. Contrasting the serum starvation-induced occurrence of apoptosis in wild-type granulosa cells, *caspase-3*-null granulosa cells deprived of hormonal support were TUNEL-negative, showed attenuated chromatin condensation by 4′,6-diamidino-2-phenylindole staining and exhibited delayed internucleosomal DNA cleavage. Such *ex vivo* findings underscore the existence of a cell autonomous (granulosa cell intrinsic) defect in apoptosis execution resulting from caspase-3 deficiency. We conclude that caspase-3 is functionally required for granulosa cell apoptosis during follicular atresia, but that the enzyme is dispensable for germ cell apoptosis in the female. (*Endocrinology* **142:** 2468–2467, 2001)

DURING PRENATAL development of the mammalian female gonads, up to two thirds of the germ cells produced during gametogenesis undergo programmed cell death (PCD) via apoptosis. This process leads to the endowment of a finite reserve of oocytes, enclosed by somatic granulosa cells as primordial follicles, at birth (1). Throughout postnatal life, these primordial follicles become activated, starting a process of follicle development through successive periods of early growth (primary and secondary or preantral follicles) followed by rapid maturation (antral follicles) to the preovulatory stage. However, the vast majority of follicles fail to complete this maturation scheme, dying en route via atresia (1, 2). Although PCD is also pivotal to the postnatal loss of oocytes due to follicular atresia, apoptosis of either the germ cell or somatic (granulosa) cell lineage can drive follicle degeneration (1). In the early stages of follicle development (primordial, primary, and small preantral), atresia is initiated by oocyte apoptosis followed by death of the granulosa cells (1, 3, 4). By comparison, atresia of maturing (late preantral, antral) and mature (subordinate preovulatory) follicles is first demarcated by scattered granulosa cell apoptosis (2, 5). As atresia progresses in these follicles, the number of dying granulosa cells increases dramatically and large masses of apoptotic bodies are shed into the antral space. Finally, the oocyte dies, and the remnants of the follicle are cleared by phagocytosis or resorption into the ovarian stroma (6, 7).

Current evidence from studies of a number of cell types indicates that the release of cytochrome *c* from mitochondria (8, 9), a key intracellular event in the PCD pathway controlled by *bcl-2* gene family members (10, 11), engages the downstream machinery needed for the execution of apoptosis. This machinery is comprised of an adapter protein termed Apaf-1 (12) that, when bound with cytochrome *c*, forms a complex with the proform of caspase-9 (13). In many cell types, caspase-9 is believed to be the most proximal enzyme in a cascade of proteolytic activity required for dismantling the cell during PCD (9, 14–16). Formation of the Apaf-1/procaspase-9 complex permits activation of the enzyme through

Received October 9, 2000.

Address all correspondence and requests for reprints to: Jonathan L. Tilly, Ph.D., Massachusetts General Hospital, VBK137C-GYN, 55 Fruit Street, Boston, Massachusetts 02114. E-mail: jtilly@partners.org.

* This work was supported by NIH Grants R01-HD-34226 and R01-AG-12279 (to J.L.T.) and Vincent Memorial Research Funds.

† Research Fellow supported by the Finnish Foundation for Pediatric Research and the Finnish Cultural Foundation.

‡ Present address: Biogen, Inc., 14 Cambridge Center, Cambridge, Massachusetts 02142.

§ Investigator with the Howard Hughes Medical Institute.

an induced proximity model (17). This biochemical step heralds the execution phase of PCD, characterized by the cleavage-activation of downstream caspase family members, such as caspase-2, -3, -6, or -7, that produce the morphological (*e.g.* cellular condensation, budding, and fragmentation, and nuclear pyknosis) and biochemical (*e.g.* DNA cleavage through nuclease activation) hallmarks of apoptosis. In addition, caspases irrevocably commit cells to death through disablement of key structural proteins, signaling factors, and nuclear enzymes required for cellular homeostasis (9, 14–16).

In the mammalian ovary, a case has been made for the existence of this PCD pathway in both oocytes and granulosa cells (1, 2). For example, a prominent role for the proapoptotic Bcl-2 family member, Bax, in activating PCD in female germ cells and follicular granulosa cells has been reported based on endogenous gene expression studies (18–21) and in-depth analyses of striking ovarian phenotypes in Bax-deficient female mice (22–24). Mitochondria, the principal intracellular targets for the actions of Bcl-2 family members (11), have been identified as direct participants in controlling oocyte apoptosis (25). In addition, mitochondrial release of cytochrome *c* has been shown to occur in murine granulosa cells during apoptosis, coincident with the processing of procaspase-3 to the active enzyme (26). Although the requirement for Apaf-1 in connecting mitochondrial cytochrome *c* release to caspase activation in ovarian cells remains to be directly established, studies documenting the accumulation of Apaf-1 protein in granulosa cells during the early stages of follicle atresia suggest that this adapter protein is indeed involved (26). Further evidence implicating caspase-3 in atresia comes from studies of gonadotropin-regulated caspase-3 messenger RNA (27) and protein (28) levels in rat granulosa cells and expression of caspase-3 in human luteinizing granulosa cells (19). We have also reported that the caspase-3-specific intracellular substrate, α-fodrin (29), is cleaved in granulosa cells during atresia (30), and that caspase inhibitors attenuate the occurrence of PCD in cultured antral follicles (30). Lastly, cleavage of a rhodamine-conjugated DEVD (Asp-Glu-Val-Asp) peptide [the preferred cleavage recognition site for caspase-3 (31)] has been shown to occur in murine granulosa cells during apoptosis *in vitro* (26).

Preliminary observations from our laboratory indicate that caspase-9, the most proximal enzyme in the execution phase of PCD, is required for apoptosis in both oocytes and granulosa cells (32). Although caspase-3 is known to be expressed in female germ cells (33), recent gene knockout studies have shown that caspase-2 [which is also expressed in oocytes (34);] is functionally required for developmental and anticancer drug-induced oocyte apoptosis (34). Nevertheless, based on observations that inhibitors of caspase-3-like enzymes prevent oocyte fragmentation induced by anticancer drugs *in vitro* (23), and that cleavage of a rhodamine-conjugated DEVD peptide occurs in oocytes during apoptosis (35), it may be that both caspase family members are needed to execute PCD in female germ cells. Herein we used *caspase-3*-null mice (36) to directly test for the functional requirement of this executioner protease in ovarian germ cell *vs.* granulosa cell demise *in vivo* and *in vitro*. The results presented herein indicate that oocytes and granulosa cells undergo PCD via genetically distinct pathways, one reliant on caspase-2 and the other dependent on caspase-3. Furthermore, we provide evidence for evolutionary conservation of caspase-3 function in the apoptosis of human granulosa cells during atresia of maturing antral follicles *in vivo* and show that an additional executioner caspase is also activated during granulosa cell demise.

Materials and Methods

Animals

Wild-type and *caspase-3*-null female mice (congenic C57BL/6) were generated by mating heterozygous (*caspase-3*$^{+/-}$) male and female mice. Offspring were genotyped by PCR analysis of tail-snip genomic DNA that amplifies the region of the *caspase-3* gene targeted by homologous recombination (36). All animal protocols were reviewed and approved by the Massachusetts General Hospital institutional animal care and use committee and were performed in strict accordance with the NIH Guide for the Care and Use of Laboratory Animals.

Human ovarian tissues

Ovarian biopsies were collected from four patients (25–35 yr of age; tissue from each patient serving as an experimental replicate) undergoing gynecological surgery for various benign conditions after informed consent and protocol approval by the Wesley Medical Center institutional review board. Ovarian tissues were fixed in 4% paraformaldehyde, embedded, sectioned (8 μm), and mounted on glass slides for histological or histochemical assessments (see below).

Mouse ovarian collection and oocyte counts

Ovaries were collected from wild-type and caspase-3-deficient female mice on day 4 postpartum and at 2 and 6 months of age. The ovaries were then fixed (0.34 N glacial acetic acid, 10% formalin, and 28% ethanol for histology, 4% paraformaldehyde for histochemistry), paraffin-embedded, serially sectioned (8 μm), and mounted in order on glass microscope slides. For histomorphometrics, the sections were stained with hematoxylin-picric acid methyl blue and analyzed for the number of healthy (nonatretic) primordial, primary, and small preantral follicles per section in every fifth section through the entire ovary, as previously described (37). Primordial follicles were identified as having a compact oocyte surrounded by a single layer of flattened (fusiform) granulosa cells, whereas primary follicles were identified as having an enlarged oocyte surrounded by a single layer of cuboidal granulosa cells. Intermediate stage follicles (compact or enlarged oocyte with a single layer of mixed fusiform and cuboidal granulosa cells) were scored as primary, because the change in granulosa cell morphology from fusiform to cuboidal is a sign that the primordial follicle is no longer quiescent. Small preantral follicles were identified as having an enlarged oocyte surrounded by at least a partial or complete second layer of cuboidal granulosa cells but no more than four layers of cuboidal granulosa cells. All oocyte-containing follicles were counted in each ovarian section scored, and each ovary was given a numerical code so that all follicle counts were conducted without knowledge of genetic background. Slides were then decoded, and the total number of healthy follicles per ovary was calculated. Follicles at the primordial, primary, and small preantral stages of development were deemed atretic if the oocyte was degenerating (convoluted and condensed, or fragmented) or absent (24, 37).

In vitro follicle cultures

Prepubertal (day 24–26 postpartum) female mice (wild-type or *caspase-3* mutant) were given a single ip injection of 10 IU equine CG (eCG; Professional Compounding Centers of America, Houston, TX), and the 8–12 largest antral (preovulatory) follicles were nonenzymatically dissected from ovaries 42 h after injection, as previously described (18, 30). Follicles were then either fixed (histology, histochemistry) or frozen (electrophoretic DNA analysis) immediately or were cultured for 12 or 24 h under serum-free conditions, as detailed previously (18, 30), before fixation or freezing.

In vitro oocyte cultures

Oocytes were isolated, cultured, and assessed for apoptosis as detailed previously (23, 34, 35, 37, 38). Briefly, wild-type or caspase-3-deficient female mice were injected with 10 IU eCG followed by 10 IU hCG (Serono Laboratories, Inc., Randolph, MA) 46 h later to induce superovulation. Mature (metaphase II) oocytes were collected from the oviducts 16 h after hCG injection and denuded of cumulus cells by a 1-min incubation in 80 IU/ml hyaluronidase (Sigma, St. Louis, MO). The oocytes were washed three times with culture medium (human tubal fluid; Irvine Scientific, Santa Ana, CA) supplemented with 0.5% (wt/vol) BSA (fraction V; Life Technologies, Inc., Grand Island, NY). Pools of 10–20 oocytes were then cultured in 0.1-ml drops of culture medium under paraffin oil in the absence or presence of 200 nM doxorubicin (Sigma). After culture, oocytes were checked for changes characteristic of apoptosis (condensation, budding, cellular fragmentation, DNA fragmentation), and the percentage of oocytes that underwent apoptosis of the total number of oocytes cultured per drop in each experiment was determined.

In vitro granulosa cell cultures

Granulosa cell cultures were carried out essentially as described previously (26). Briefly, immature (21–24 days postpartum) wild-type and caspase-3-deficient female mice were injected with 10 IU eCG. Forty-two hours later, ovaries were dissected out and decapsulated, and the stimulated follicles were punctured with fine needles to collect the granulosa cells into Waymouth's MB752/1 medium (Life Technologies, Inc.) supplemented with 100 U/ml penicillin, 100 μg/ml streptomycin, and 0.29 mg/ml L-glutamine. After trypan blue staining analysis, approximately 3×10^5 viable cells were cultured in 35 $\times$ 10-mm dishes containing 2 ml culture medium for 24 or 48 h with 10% FBS (HyClone Laboratories, Inc., Logan, UT). The medium and nonadherent cells were removed, fresh serum-free culture medium (2 ml) was added, and the cells were maintained for an additional 48 or 24 h, respectively (total length of culture was 72 h in both cases), to induce apoptosis. At the termination of culture, granulosa cells were fixed with 4% paraformaldehyde for 30 min at 20 C, stained for 10 min with 4′,6-diamidino-2-phenylindole (DAPI; Sigma) at a final concentration of 30 μg/ml, and then stored at 4 C until examined by fluorescence microscopy using an UV light filter to detect nuclear chromatin condensation and fragmentation characteristic of apoptosis (26). In each experiment, over 1×10^3 granulosa cells in randomly chosen fields were scored for the occurrence of nuclear condensation *vs.* fragmentation (of the total number of cells present).

DNA isolation, radiolabeling, and gel electrophoretic analysis

Genomic DNA was extracted, quantitated, and 3′-end labeled with [α-^{32}P]dideoxy-ATP (3000 Ci/mmol; Amersham Pharmacia Biotech, Piscataway, NJ) using terminal deoxynucleotidyl transferase (Roche Molecular Biochemicals, Indianapolis, IN), as previously described (39, 40). Radiolabeled samples were resolved through 2% agarose gels, and the extent of internucleosomal cleavage was assessed by autoradiography.

Terminal deoxynucleotidyl transferase-mediated dUTP nick end labeling (TUNEL)

The occurrence of apoptosis in ovarian and follicle sections was assessed, as described previously (40), by monitoring the presence of DNA fragmentation *in situ*. Slides were analyzed by conventional light microscopy after light counterstaining with hematoxylin. Cells exhibiting dark brown staining from the colorimetric reaction were considered positive for DNA fragmentation. Negative controls, conducted by omitting the labeling enzyme, yielded no reaction product (data not shown).

Immunohistochemistry

Paraffin-embedded sections (6 μm for follicles or 8 μm for ovaries) were analyzed by immunohistochemistry without (follicle sections) or with (mouse and human ovarian sections) high temperature antigen unmasking, as previously described (26, 37, 41, 42). Briefly, after peroxidase quenching [and microwave treatment if employed (42)], sections were incubated with a 1:3000 dilution of the cleaved caspase-3 antibody (CM1) (43) for 1 h at room temperature or with a 1:100 dilution of the cleaved caspase-7 antibody (Cell Signaling Technology/New England Biolabs, Inc., Beverly, MA) overnight at 4 C. Sections were washed and then incubated with a 1:200 dilution of biotinylated goat antirabbit Ig antibody (Calbiochem-Novabiochem, La Jolla, CA) for 1 h at room temperature. Sections were washed, incubated for 45 min at room temperature with horseradish peroxidase-conjugated streptavidin, washed, and reacted with ice-cold 0.5 mg/ml 3,3′-diaminobenzidine with 0.03% hydrogen peroxide at room temperature for antigen detection. Sections were then counterstained with hematoxylin and analyzed by light microscopy.

Immunocytochemistry

Granulosa cells harvested from gonadotropin-primed mice were cultured for 24 h with 10% FBS as described above (see *In vitro granulosa cell cultures*). The medium and nonadherent cells were removed, and 2 ml fresh serum-free culture medium were added. The cells were then maintained for an additional 48 h to induce apoptosis. At the termination of the culture, medium and nonadherent cells were removed, after which 1 ml 3% neutral-buffered paraformaldehyde was added to the dish. Following fixation for 10 min at 4 C, immunocytochemical staining was carried out using the CM1 antibody essentially as previously described (43) or the cleaved caspase-7 antibody (Cell Signaling Technology/New England Biolabs, Inc.) according to the manufacturer's instructions. In brief, the cells were permeabilized for 10 min at −20 C in 100% methanol and blocked with buffer containing 5.5% normal goat serum. The cells were then incubated with a 1:1000 (CM1) or 1:100 (cleaved caspase-7) dilution of primary antibody for 1 h at room temperature (CM1) or 15 h at 4 C (cleaved caspase-7). The cells were washed and incubated with a 1:200 dilution of biotinylated goat antirabbit Ig antibody for 1 h at room temperature. The cells were washed again and incubated for 45 min at room temperature with horseradish peroxidase-conjugated streptavidin. After washing, the cells were finally reacted with an ice-cold preparation (0.5 mg/ml) of 3,3′-diaminobenzidine in the presence of 0.03% hydrogen peroxide at room temperature for antigen detection. Cells were then lightly counterstained with hematoxylin and analyzed by light microscopy.

Data presentation and statistical analysis

Each experiment was independently replicated at least three times with different mice in each experiment. All graphs represent the mean $\pm$ SEM of combined data from the replicate experiments, whereas representative photomicrographs are presented for histology, histochemistry, cytochemistry, and autoradiography (see figures and tables for more details). For quantitative analyses, Student's *t* test was used for comparison of mean values obtained with wild-type *vs. caspase-3*-null mice, and a $P < 0.05$ was chosen to indicate a statistically significant difference.

Results

Oocyte endowment in neonatal caspase-3 mutants

As the size of the oocyte reserve set forth at birth reflects the magnitude of apoptosis in the developing fetal ovarian germ line (1), we first examined follicular endowment in wild-type and caspase-3-deficient female mice on day 4 postpartum. These experiments revealed a normal ovarian architecture in both groups (data not shown), with no significant differences in the numbers of nonatretic primordial, primary or small preantral follicles present in wild-type *vs.* mutant female littermates (Fig. 1A).

In vitro apoptosis in caspase-3-deficient germ cells

To directly test for potential defects in germ cell apoptosis, denuded oocytes collected from wild-type or caspase-3-

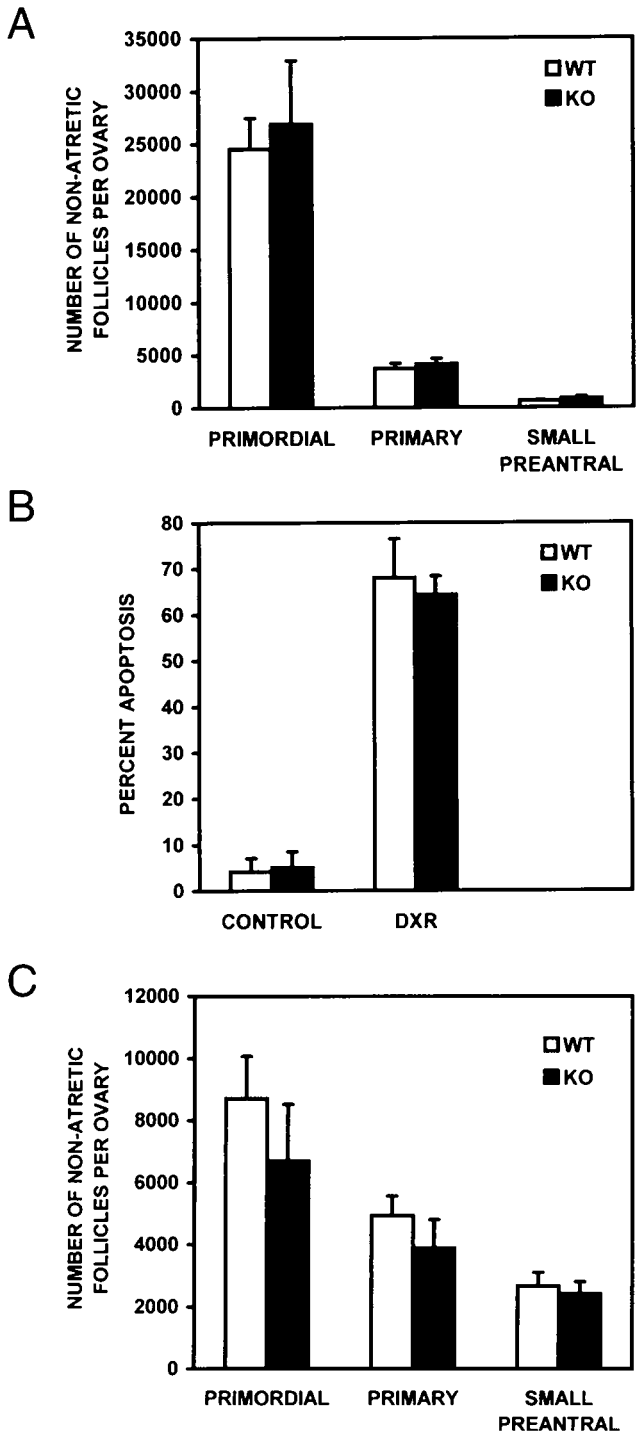

FIG. 1. Caspase-3 is not required for apoptosis in oocytes. A, Histomorphometric analysis of the numbers of nonatretic primordial, primary, and small preantral follicles in ovaries of wild-type (WT) and *caspase-3* gene knockout (KO) female mice on day 4 postpartum (mean ± SEM; n = 4 mice/genotype). B, Apoptotic response of wild-type (WT) and caspase-3-deficient (KO) oocytes treated without (control) or with 200 nM DXR for 24 h (mean ± SEM of results from 3 independent experiments using 10–20 oocytes from each genotype per treatment group in each experiment). C, Numbers of nonatretic primordial, primary, and small preantral follicles remaining in the ovaries of wild-type (WT) or *caspase-3*-null (KO) female mice at 2 months of age (mean ± SEM; n = 4 mice/genotype). No statistical differences were observed for any end point comparing wild-type *vs. caspase-3* mutant mice.

deficient females were treated *in vitro* with 200 nM of the anticancer drug, doxorubicin (DXR) (23, 34). After superovulation by exogenous gonadotropin priming, the numbers of oocytes ovulated in *caspase-3*-null females was twice that observed in wild-type females (42 ± 9 *vs.* 20 ± 9 oocytes/mouse, respectively; mean ± SEM; n = 3–4 mice/genotype); however, this difference was not statistically significant ($P = 0.14$, by Student's t test). The apoptotic response of *caspase-3*-null oocytes to DXR exposure *in vitro* was not different from that of wild-type oocytes cultured in parallel with the drug for 12, 24, or 48 h (Fig. 1B; data not shown for 12 or 48 h points). In addition, the low rate of spontaneous oocyte apoptosis (no drug treatment) *in vitro* was unaffected by the absence of caspase-3 (Fig. 1B).

Histomorphometric evaluation of follicle numbers in adult caspase-3 mutants

Previous studies have shown that Bax-deficient female mice are born with a normal endowment of primordial follicles at birth, but possess 3-fold more primordial follicles in young adult life. This phenotype was determined to be the result of defects in postnatal oocyte death leading to attenuated atresia of primordial and primary follicles (24). Based on these observations, we next tested whether a similar situation exists in *caspase-3* mutant females. At 2 months of age, however, young adult wild-type and *caspase-3*-null females were found to possess comparable numbers of nonatretic primordial, primary, and small preantral follicles in their ovaries (Fig. 1C).

Immunolocalization of cleaved (activated) caspase-3 in the mouse ovary

To determine whether active caspase-3 was present and correlated with somatic cell apoptosis in the ovary *in vivo*, immunohistochemistry was performed using a rabbit polyclonal antiserum (CM1) that recognizes the p18 subunit of cleaved caspase-3 but not the zymogen form of the enzyme (43). As a model, wild-type prepubertal female mice were killed immediately (0 h; moderate level of early antral follicle atresia) or were given a single injection of eCG, then killed 48 h later (preovulatory follicle development, no atresia) or 96 h later (atresia of the preovulatory cohort developed 48 h earlier) (44, 45). In mice before gonadotropin injection, ovaries contained seven to nine maturing follicles per section with granulosa cells labeled by the CM1 antibody (Fig. 2A) and three to five maturing follicles per section with granulosa cells labeled by TUNEL (to detect DNA cleavage associated with apoptosis; Fig. 2B). At 48 h post-eCG injection, we could not detect CM1 immunoreactivity (Fig. 2C) or TUNEL staining in any of the antral follicles (Fig. 2D), consistent with the ability of eCG priming to suppress caspase-3 expression (26, 27) and antral follicle atresia (18, 43, 44) in the prepubertal rodent ovary. At 96 h post-eCG, granulosa cells of the now atretic cohort of antral follicles induced to undergo preovulatory development 48 h earlier by eCG priming were again characterized by CM1 immunoreactivity (Fig. 2E) and TUNEL staining (Fig. 2F).

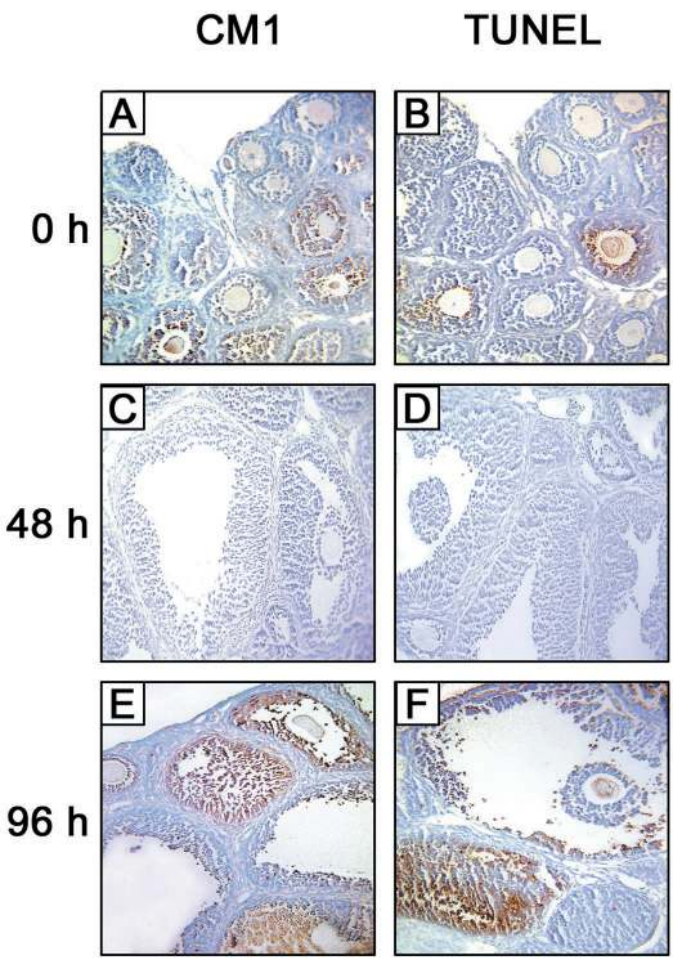

FIG. 2. Immunolocalization of processed caspase-3 during granulosa cell apoptosis and atresia in the mouse ovary *in vivo*. A and B, Representative histochemical analysis of CM1 immunostaining (cleaved caspase-3; A, C, and E) or TUNEL analysis of DNA cleavage (apoptosis; B, D, and F) in ovaries of prepubertal female mice before gonadotropin stimulation (0 h; A and B) or 48 h (C and D) or 96 h (E, F) after eCG injection. Original magnifications, ×200. These data are representative of results obtained from analyzing each end point using ovaries from at least three different mice under each experimental condition. In each experiment, three to six sections from each ovary were assessed for either CM1 immunoreactivity or TUNEL.

Caspase-3 activation in granulosa cells during apoptosis in vitro

The occurrence of procaspase-3 processing in granulosa cells during apoptosis was further investigated by immunocytochemical staining of granulosa cells starved of serum *in vitro*. Processed caspase-3 was readily detected in granulosa cells that already exhibited (Fig. 3, A and B), as well as those just initiating (Fig. 3, C and D), cellular condensation associated with apoptosis.

Ovarian histology and apoptosis assessments in adult caspase-3-deficient mice

In light of the positive correlation observed between CM1 immunoreactivity and apoptosis in granulosa cells, we histologically surveyed ovaries from adult (2–6 months of age) caspase-3-deficient females for potential defects in maturing follicle atresia. Contrasting with the ovarian architecture observed in adult wild-type females (Fig. 4, A–C), ovaries from all adult *caspase-3* gene knockout mice were characterized by the presence of aberrant atretic follicles exhibiting a shrunken or disorganized appearance without or with blood cell infiltration (Fig. 4, D–F). In many instances, the oocytes had either spontaneously activated (resumed meiosis) or degenerated. Histochemical assays of *caspase-3* mutant ovarian sections revealed the persistence of granulosa cells in these follicles that failed to be eliminated by apoptosis. This was concluded based on the absence of TUNEL-positive staining for the occurrence of DNA cleavage (Fig. 5, E and F; compare with wild-type in Fig. 5, A and B) and on the absence of nuclear pyknosis as determined by DAPI staining of nuclear morphology (Fig. 5G; compare with wild-type in Fig. 5C). Quantitative analysis of randomly selected sections prepared from ovaries of three mice per genotype revealed 3.6 ± 0.2 TUNEL-positive follicles/ovarian section in wild-type mice (118 TUNEL-positive follicles of 33 sections scored). By comparison, we detected only 0.8 ± 0.1 TUNEL-positive follicles per ovarian section in *caspase-3*-null mice (29 TUNEL-positive follicles of 36 sections scored; $P < 0.001$). When analyzed using the CM1 antibody, granulosa cells within atretic follicles of caspase-3-deficient mice showed light cytoplasmic staining with only a single granulosa cell, on occasion, being labeled more intensely (Fig. 5H). This pattern contrasted with the immunoreaction observed in the majority of granulosa cells within atretic follicles of wild-type mice (Figs. 2 and 5D).

In vitro follicle cultures

To further study the defective apoptosis of caspase-3-deficient granulosa cells during atresia, we isolated pools of nonatretic antral (preovulatory) follicles from wild-type and caspase-3-deficient mice and cultured these follicles *ex vivo* without hormonal support to induce atresia (18, 45, 46). Regardless of genotype, follicles analyzed immediately after isolation were indistinguishable by histological assessments (Fig. 6, A and B), histochemical assays (Fig. 6, E, F, I, and J), and gel electrophoretic analysis of DNA integrity (Fig. 7). After *in vitro* culture without hormonal support for 12 h, granulosa cells within wild-type follicles displayed all of the expected features of apoptosis, including cellular condensation and detachment (Fig. 6C), DNA cleavage (Figs. 6K and 7), and formation of large numbers of apoptotic bodies (Fig. 6C). By comparison, all of these events were either markedly attenuated or absent in granulosa cells of *caspase-3*-null follicles cultured in parallel (Fig. 6, D and L, and Fig. 7). Furthermore, the pattern of CM1 immunoreactivity in follicles induced to undergo atresia *in vitro* was similar to that observed for atresia *in vivo* (Figs. 2 and 5). The intense CM1 immunoreactivity detected in granulosa cells of wild-type follicles cultured *in vitro* (Fig. 6G) was markedly reduced, but not entirely absent, in granulosa cells of caspase-3-deficient follicles incubated in parallel (Fig. 6H). By 24 h of culture, it became increasingly difficult to distinguish differences in granulosa cells of wild-type *vs.* caspase-3-deficient follicles by morphology and TUNEL (data not shown) and by gel electrophoretic analysis of DNA (Fig. 7).

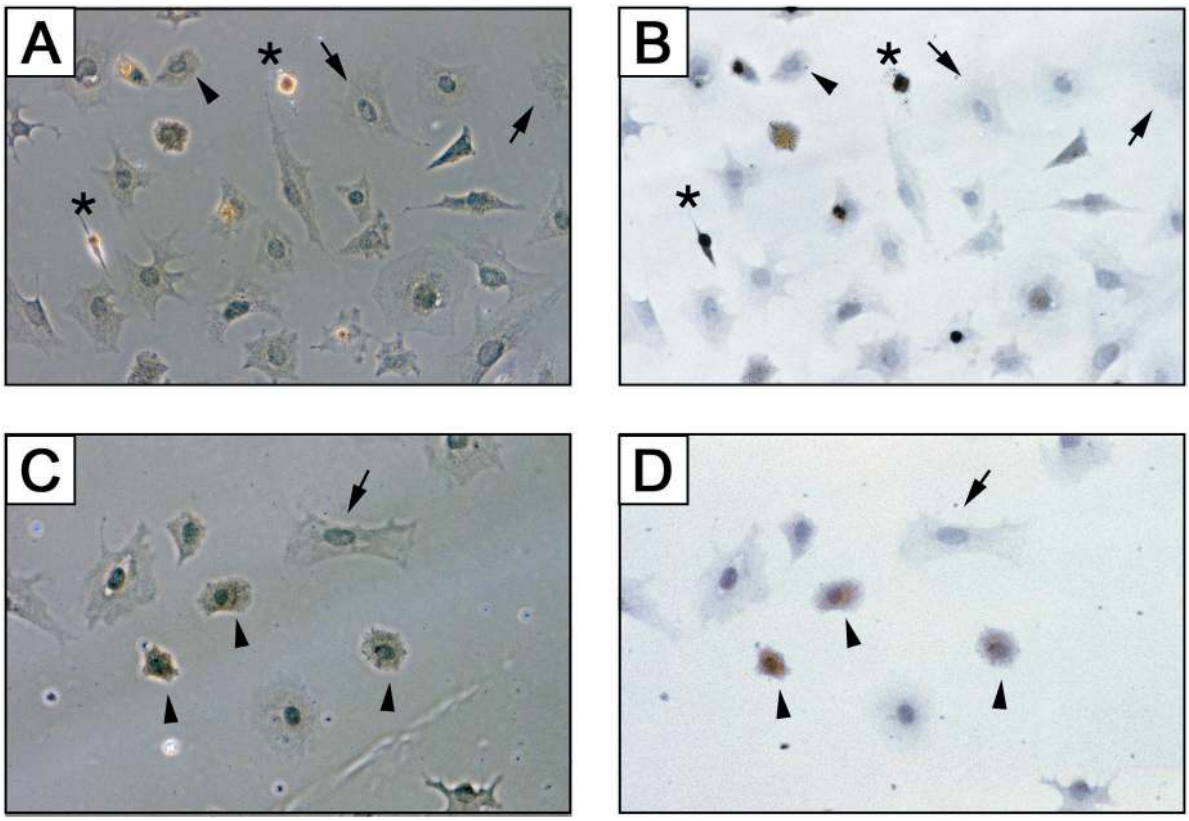

FIG. 3. Caspase-3 activation in murine granulosa cells during apoptosis induced *in vitro*. Phase contrast (A and C) and brightfield (B and D) images of wild-type granulosa cells cultured for 48 h without serum followed by immunocytochemical staining for the presence of cleaved caspase-3. Cleaved caspase-3 was absent in some morphologically normal granulosa cells (*arrows*), but was detected in other morphologically normal (*arrowheads*) granulosa cells as well as in apoptotic (condensed) granulosa cells (*asterisks*). Original magnifications, ×400. These findings are representative of results obtained in three independent experiments conducted, using different mice for each experiment.

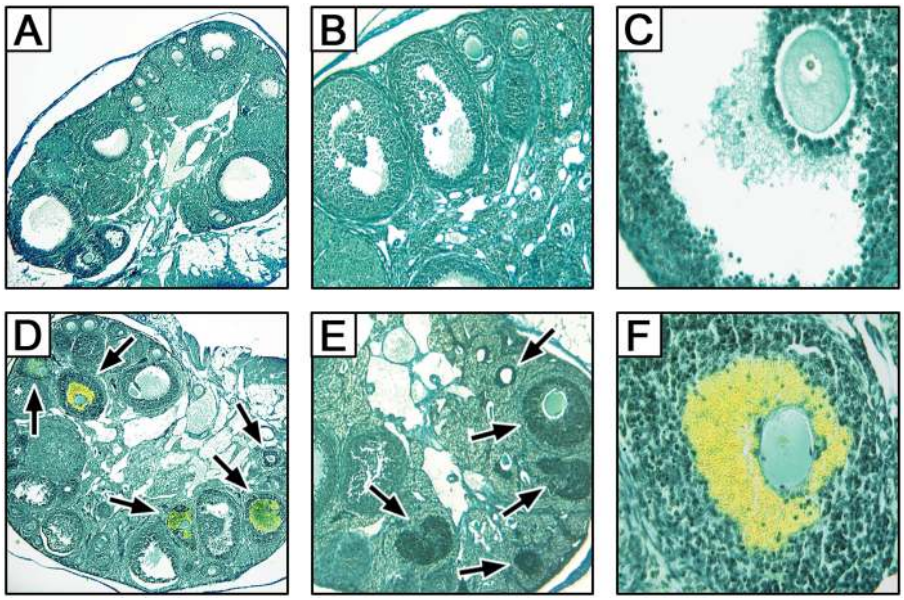

FIG. 4. Caspase-3 loss of function leads to defective atresia of maturing follicles *in vivo*. Representative histology of wild-type (A–C) and *caspase-3*-null (D–F) ovaries in young adult female mice, as viewed by picric acid methyl blue staining, which highlights blood cells in *yellow*. *Arrows* point to the aberrant follicles in the *caspase-3* mutants. Original magnifications: A and D, ×100; B and E, ×200; C and F, ×400. These data are representative of results obtained from the analysis of at least four mice per genotype.

In vitro granulosa cell cultures

To further elucidate the consequences of caspase-3 deficiency, granulosa cells from wild-type and *caspase-3* mutant mice were isolated and placed in serum-free cultures. Wild-type granulosa cells starved of hormonal support initiated apoptosis, as determined by the occurrence of nuclear condensation and chromatin fragmentation (Fig. 8, A and B). By comparison, caspase-3-deficient granulosa cells cultured in parallel frequently exhibited abnormal clumping of DNA into a single mass of partially condensed nuclear material

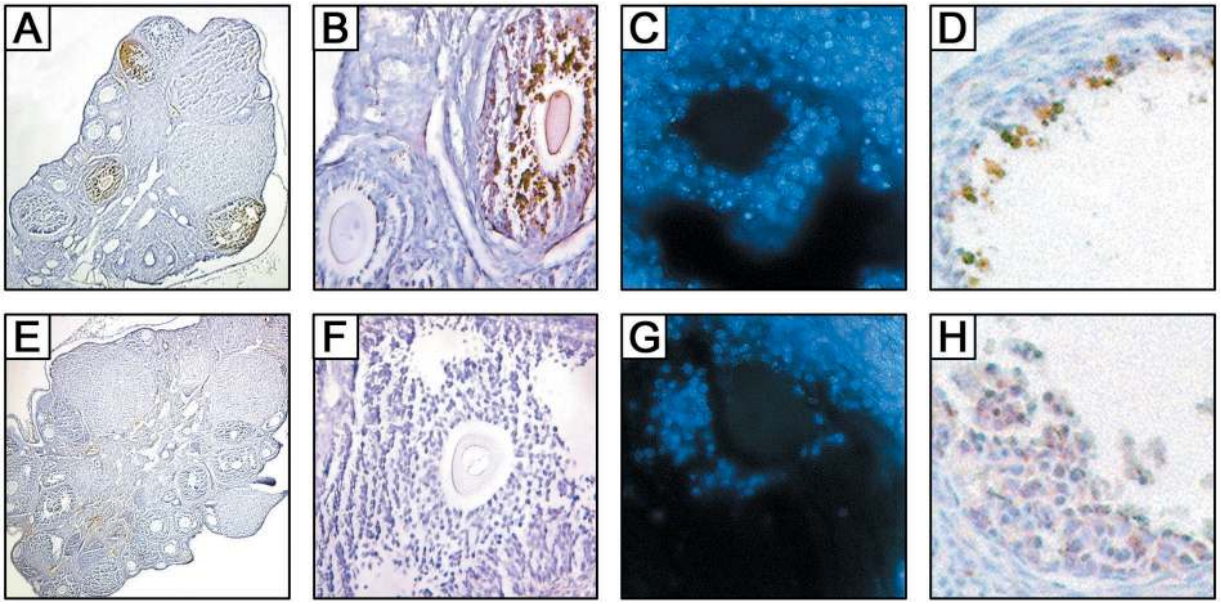

FIG. 5. Caspase-3 gene inactivation leads to aberrant granulosa cell death during atresia of maturing follicles *in vivo*. Low and high power magnifications of ovaries collected from adult wild-type (A and B) or caspase-3-deficient (E and F) female mice after TUNEL to identify DNA cleavage associated with apoptosis (*brown* reaction product). High power magnifications of nuclear morphology (DAPI staining) in atretic follicles of wild-type (C) and *caspase-3* mutant (G) mice confirm the defective apoptosis (nuclear pyknosis) of granulosa cells during atresia *in vivo* resulting from caspase-3 loss of function. D and H, Immunohistochemical analysis of processed caspase-3 (CM1 staining) in granulosa cells of atretic follicles of wild-type (D) and *caspase-3*-null (H) adult female mice. Original magnifications: A and E, ×100; B and F, ×400; C, D, G, and H, ×600. These data are representative of results obtained from the analysis of each end point using at least four mice per genotype. For the TUNEL analysis, at least 10 randomly selected sections from each ovary were analyzed, and the quantitative results are presented in the text (see *Results*).

(Fig. 8, C and D). By scoring over 1×10^3 granulosa cells in randomly chosen fields for the occurrence of nuclear condensation *vs.* fragmentation, we determined that caspase-3-deficient granulosa cells were defective in their capacity to complete the process of nuclear fragmentation after the initial condensation of DNA (Table 1).

Caspase-7 activation in wild-type and caspase-3-deficient granulosa cells during apoptosis

As the death of granulosa cells in caspase-3-deficient mice was defective, but not absent, other downstream caspases (*e.g.* caspase-2, -6, and/or -7) probably also function as mediators of ovarian somatic cell demise. In addition, the presence of low levels of CM1 immunoreactivity in caspase-3-deficient granulosa cells suggests that the antibody is selective, but not entirely specific, for the cleaved form of caspase-3. Previous work has shown that caspase-3 and caspase-7 are similar in many respects, including substrate cleavage preferences and catalytic properties (31, 47). Therefore, in the next series of experiments we used a recently developed antibody that recognizes the cleaved form of caspase-7 to study its expression patterns in wild-type and *caspase-3* mutant granulosa cells during apoptosis induced by serum-free culture *in vitro*. Regardless of genotype, we detected the activated form of caspase-7 in those granulosa cells that had initiated cellular condensation associated with apoptosis (Fig. 9).

Immunolocalization of cleaved caspase-3 and cleaved caspase-7 in human ovaries

To provide evidence that the proapoptotic function of caspase-3 and/or caspase-7 in granulosa cells was evolutionarily conserved, adult human ovarian biopsies were processed by serial section analysis for four separate end points in each follicle: histology, CM1 (cleaved caspase-3) immunoreactivity, cleaved caspase-7 immunoreactivity, and TUNEL for DNA cleavage. Our collection of human ovarian biopsies did not contain any nonatretic antral follicles; however, in nonatretic immature (primordial, primary) follicles, we failed to detect evidence of cleaved caspase-3, cleaved caspase-7, or DNA cleavage (data not shown). In antral follicles at the earliest stages of atresia (very few pyknotic granulosa cells per section; Fig. 10A), caspase-3 processing was the first sign of pending granulosa cell death (Fig. 10B) with low or no staining of granulosa cells by TUNEL (Fig. 10D). Additionally, processed caspase-7 was not detected in granulosa cells of follicles at these earliest stages of atresia (Fig. 10C). As atresia progressed (granulosa cell disorganization, increased numbers of pyknotic cells; Fig. 10E), CM1 immunoreactivity and TUNEL staining became much more pronounced (Fig. 10, F and H), and processed caspase-7 became detectable (Fig. 10G). In grossly atretic follicles (nearly complete dissolution of the granulosa cell layers, shedding of apoptotic bodies into the antral space; Fig. 10I), CM1 and cleaved caspase-7 immunoreactivity remained high in dying/dead granulosa cells, and CM1 immunoreactivity be-

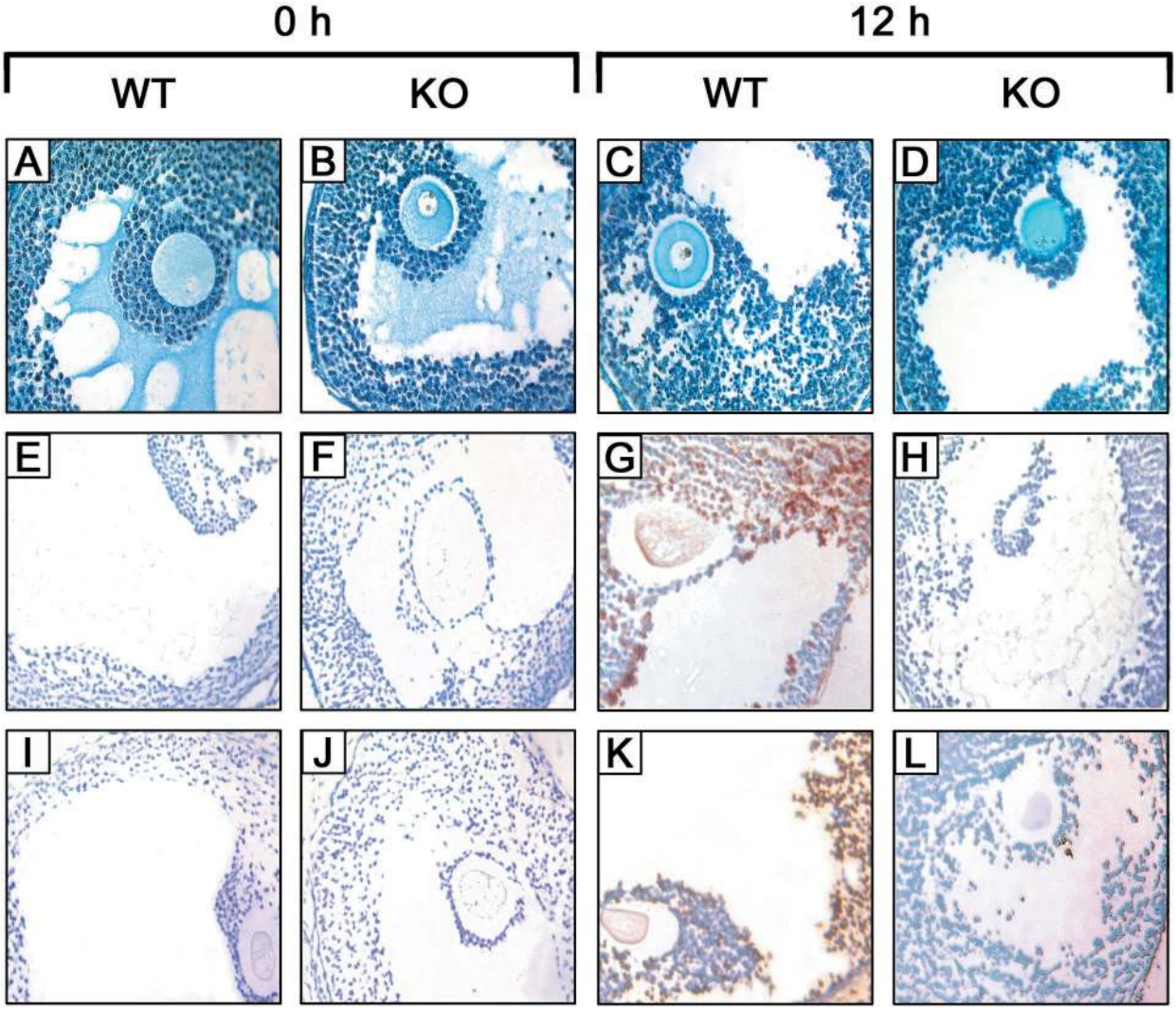

FIG. 6. Defective apoptosis of granulosa cells in caspase-3-deficient antral follicles cultured *in vitro*. A–D, Histology of wild-type (WT) and *caspase-3*-null (knockout, KO) follicles before serum-free culture (0 h) or after a 12-h culture without serum or hormones to induce atresia. E–H, Immunohistochemical staining (*dark brown* reaction product) of wild-type and caspase-3-deficient follicles for processed caspase-3 using the CM1 antibody before and after a 12-h culture. I–L, Analysis of DNA cleavage by TUNEL (*dark brown* reaction product) in wild-type and caspase-3-deficient follicles before and after a 12-h culture. Original magnifications, ×400. These data are representative of results obtained from the analysis of each end point using between two and six follicles per experimental group per genotype with each experiment repeated on three separate occasions.

came detectable in the adjacent theca-interstitial cells (Fig. 10J).

Discussion

Significant progress has been made over the past several years in elucidating the cell and molecular biology of apoptosis in the ovary (1, 2). Although the list of factors proposed to be involved in regulating cell fate in the ovary has grown considerably, very little is known of cell lineage specificity for programmed cell death signaling in the female gonads. Recently, it was reported that targeted disruption of the *caspase-2* gene in mice leads to a striking defect in the ability of ovarian germ cells to execute apoptosis in response to developmental cues or pathological insults (34). By comparison, knockout of the gene encoding *bax*, a proapoptotic member of the *bcl-2* gene family expressed in oocytes and granulosa cells (18–21), disrupts apoptosis in both ovarian cell lineages (22–24). Recent preliminary studies indicate that caspase-9 is also functionally required for the execution of PCD in both oocytes and granulosa cells of the mouse ovary (32), collectively suggesting that divergence in how germ cells *vs.* granulosa cells execute PCD would be before Bax function or after caspase-9 activation. As caspase-9 is known to initiate the execution phase of apoptosis by cleavage-activation of downstream effector caspases, such as caspase-2, -3, -6, and -7, herein we sought to determine whether the PCD pathway in oocytes and granulosa cells diverges at a step distal to caspase-9 activation.

One possibility, supported in part by the scientific literature, is that caspase-2 is required for oocyte apoptosis (34), but is dispensable for granulosa cell demise. Indeed, we have recently observed that atresia of maturing antral follicles, a

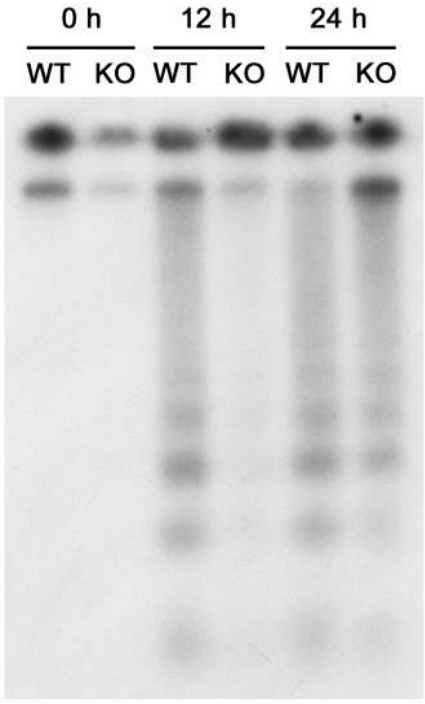

FIG. 7. Delayed internucleosomal DNA cleavage in caspase-3-deficient antral follicles cultured *in vitro*. Representative (from 3 independent experiments using 6–14 follicles/treatment group per genotype in each experiment) autoradiographic analysis of DNA integrity in wild-type (WT) or *caspase-3*-null (knockout, KO) follicles before (0 h) or after a 12- or 24-h culture without hormonal support to induce granulosa cell death and atresia. Note the markedly delayed occurrence of internucleosomal DNA cleavage in granulosa cells of *caspase-3* mutant follicles at 12 h.

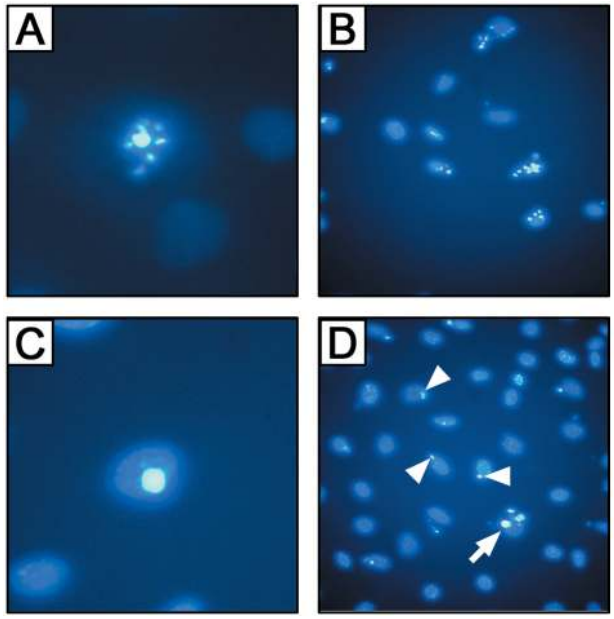

FIG. 8. Essential contribution of caspase-3 to apoptosis-associated nuclear changes in cultured granulosa cells. Representative example of abnormal nuclear collapse (partially compacted, nonfragmented chromatin) during apoptosis of caspase-3-deficient granulosa cells (C), compared with the tightly condensed and highly fragmented chromatin in wild-type granulosa cells (A), after a 24-h serum-free culture. Although some caspase-3-deficient granulosa cells show eventual fragmentation of their nuclei by 48 h of culture (designated by *arrow* in D), many cells remain defective (designated by *arrowheads* in D) compared with wild-type granulosa cells cultured for 48 h in parallel (B). Original magnifications, ×400. These data are representative of results from three independent experiments using one to three mice per genotype in each experiment to harvest the granulosa cells for culture (see also Table 1).

process driven by granulosa cell apoptosis, proceeds normally in *caspase-2* mutant female mice (unpublished observations). As *caspase-7* gene knockout is lethal (16), and generation of *caspase-6* gene knockout mice remains as yet reported (16), we focused our attention on mice lacking the principal executioner caspase activated by caspase-9, that being caspase-3 (36). This particular enzyme was a logical candidate for investigation in the context of granulosa cell apoptosis based on previous findings of an inverse correlation between caspase-3 expression (messenger RNA and protein) and apoptosis in granulosa cells of the rat ovary (27, 28). Furthermore, procaspase-3 processing and caspase-3-like enzymatic activity have been detected in murine granulosa cells during apoptosis (26), and cell-permeant peptide inhibitors selective for caspase-3 (*e.g.*, zDEVD-fmk) suppress granulosa cell death in cultured ovarian follicles of the mouse (30). However, the fact that oocytes express both caspase-2 (34) and caspase-3 (33) coupled with reports that caspase-3-selective inhibitors repress oocyte death (23) and that caspase-3-like enzymatic activity is detectable in dying oocytes (35) raised the possibility that oocytes use both executioner caspases to complete PCD.

Our first series of experiments failed to provide evidence supporting a functional requirement for caspase-3 in germ cell apoptosis. Contrasting the increased number of primordial and primary follicles endowed in *caspase-2* mutant females due to defective apoptosis in oocytes during prenatal ovarian development (34), caspase-3-deficient female mice were born with comparable numbers of oocyte-containing follicles as their wild-type female siblings. Other studies from our laboratory have shown that *bax* mutant female mice are not born with more oocytes, but possess an excess number of primordial and primary follicles in young adult life due to defects in oocyte apoptosis associated with atresia at these early stages of follicle development (24). Thus, defects in oocyte death due to a gene knockout can become apparent

TABLE 1. Analysis of nuclear changes in wild-type and *caspase*-3 mutant granulosa cells during apoptosis induced by serum-free culture

Culture time/genotype	Nuclear morphology		
	Normal	Condensed	Fragmented
24 h/wild-type	86.1 ± 1.6	10.7 ± 1.2	3.2 ± 1.0
24 h/mutant	89.2 ± 1.1	10.4 ± 1.1	0.4 ± 0.2[a]
48 h/wild-type	72.3 ± 1.8	14.3 ± 1.7	13.5 ± 1.4
48 h/mutant	79.7 ± 1.2[a]	14.4 ± 1.2	5.9 ± 0.9[b]

All values, provided as a percentage of the total number of cells counted, represent the mean ± SEM of combined results from three independent experiments with different mice used to prepare the cells in each experiment. For each group, at least 1×10^3 cells in random fields were scored. See Fig. 8 for representative photomicrographs of the various nuclear morphologies.

[a] $P = 0.009$ *vs.* wild-type.

[b] $P < 0.001$ *vs.* wild-type.

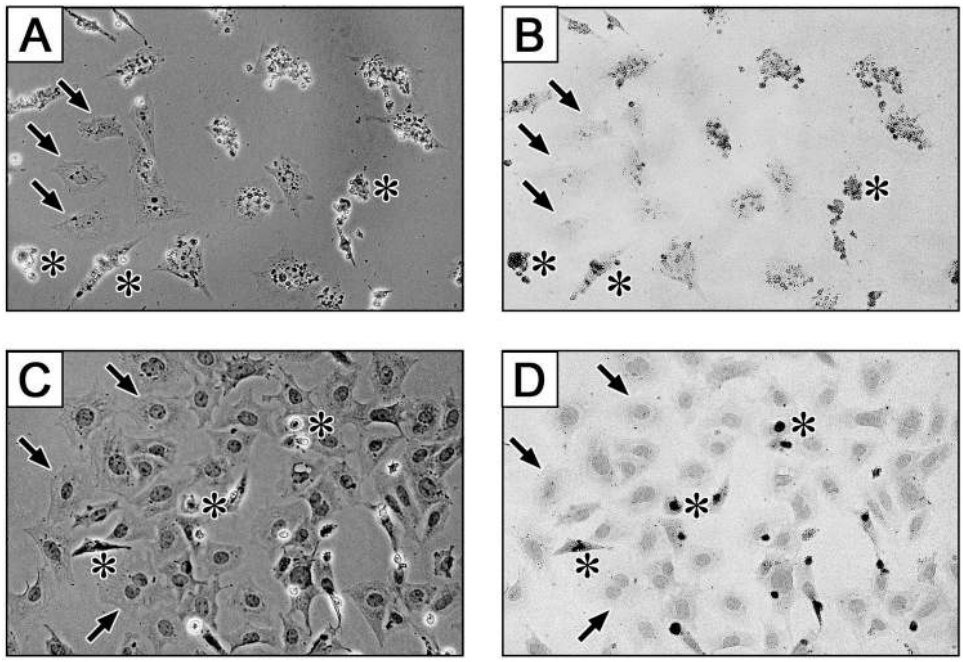

FIG. 9. Caspase-7 activation in wild-type and *caspase-3* mutant granulosa cells during apoptosis *in vitro*. Phase contrast (A and C) and brightfield (B and D) images of wild-type (A and B) and caspase-3-deficient (C and D) granulosa cells, cultured for 48 h without serum, analyzed by immunocytochemistry for the presence of cleaved caspase-7. Regardless of genotype, a positive correlation between cellular condensation (apoptosis; A and C) and caspase-7 activation (B and D) was observed (the condensed cells designated by *asterisks* in A and C are the same cells showing cleaved caspase-7 immunoreactivity in B and D). Morphologically normal cells (*arrows*) showed little or no cleaved caspase-7 immunoreactivity. Original magnifications, ×400. These findings are representative of results obtained in three independent experiments using different mice for each experiment.

in either prenatal (*caspase-2* mutant) or postnatal (*bax* mutant) life. Nonetheless, this latter possibility was not the case with caspase-3-deficient females based on our observations that follicle numbers in wild-type and mutant females were not different in young adult life. Moreover, and again in contrast to *caspase-2*-null oocytes (34), caspase-3-deficient oocytes failed to show resistance to anticancer drug-induced apoptosis *in vitro*. In further support of these findings, microinjection of active recombinant caspase-3 (30) into murine oocytes does not trigger apoptosis (G. I. Perez and J. L. Tilly, unpublished data) despite the fact that microinjection of recombinant Bax, an upstream activator of the caspase cascade, induces oocyte death (38). These latter observations are consistent with recent data derived from studies of neurons microinjected with various recombinant caspases in which some, but not all, of the caspases tested induced apoptosis (48). Collectively, these data, which show that expression of gene product (*i.e.*, caspase-3 in oocytes) (33) does not always equate to functional importance in a given cellular response (*i.e.*, apoptosis), underscore the importance of evaluating gene mutant mice.

Our next set of experiments using an antibody (CM1) that recognizes the cleaved form of caspase-3 (43) demonstrated a positive correlation between CM1 immunoreactivity and apoptosis in granulosa cells both *in vivo* and *in vitro*. Such findings are in accordance with published observations implicating caspase-3 in granulosa cell death (19, 26–28, 30). That the active caspase-3 enzyme recognized by the CM1 antibody is a key functional participant in the granulosa cell death program was supported by the presence of aberrant atretic follicles in caspase-3-deficient mouse ovaries. These follicles were characterized by the persistence of granulosa cells that failed to be properly eliminated by apoptosis, as confirmed by assessments of cellular morphology, TUNEL for DNA cleavage and DAPI staining for nuclear condensation. To further examine this phenotype under controlled experimental conditions that resemble atresia *in vivo*, we studied the progression of granulosa cell apoptosis in antral follicles isolated from gonadotropin-primed immature mice and placed in serum-free cultures. These experiments underscored the abnormal or attenuated progression of many apoptotic events in *caspase-3*-null granulosa cells, including defective nuclear collapse (an end point further confirmed with the granulosa cell cultures), the absence of cellular shrinkage and budding to generate apoptotic bodies, and delayed genome fragmentation. The inability of caspase-3-deficient granulosa cells to fully execute PCD is in agreement with the reported role of caspase-3 in degradation of cytoskeletal proteins leading to cellular shrinkage as well as in cleaving nuclear scaffold proteins and activating nucleases required for chromatin condensation (14–16, 29, 49).

We would point out that the lack of functional caspase-3 in granulosa cells, although causative of many defects in the temporal execution or progression of events normally associated with apoptosis, did not prevent the eventual death of granulosa cells *in vitro* or *in vivo*. This point is most clearly shown by results from the follicle culture studies, in which the striking differences in dying granulosa cells of wild-type *vs. caspase-3*-null follicles cultured for 12 h became difficult to discern when the cultures were allowed to progress for 24 h. Moreover, the nearly complete absence of nuclear fragmentation in caspase-3-deficient granulosa cells starved of hormonal support for 24 h (compared with the significantly higher incidence of nuclear fragmentation in the wild-type cells cultured in parallel) became less pronounced as the cultures were continued for up to 48 h. These findings are in keeping with recent data derived from studies of hepatocytes and thymocytes lacking caspase-3. These cells were reported exhibit abnormal morphological changes and delayed DNA fragmentation after Fas activation, but the cells still eventually died (50). Nonetheless, the *in vivo* significance of delayed granulosa cell death in follicles attempting to undergo atresia

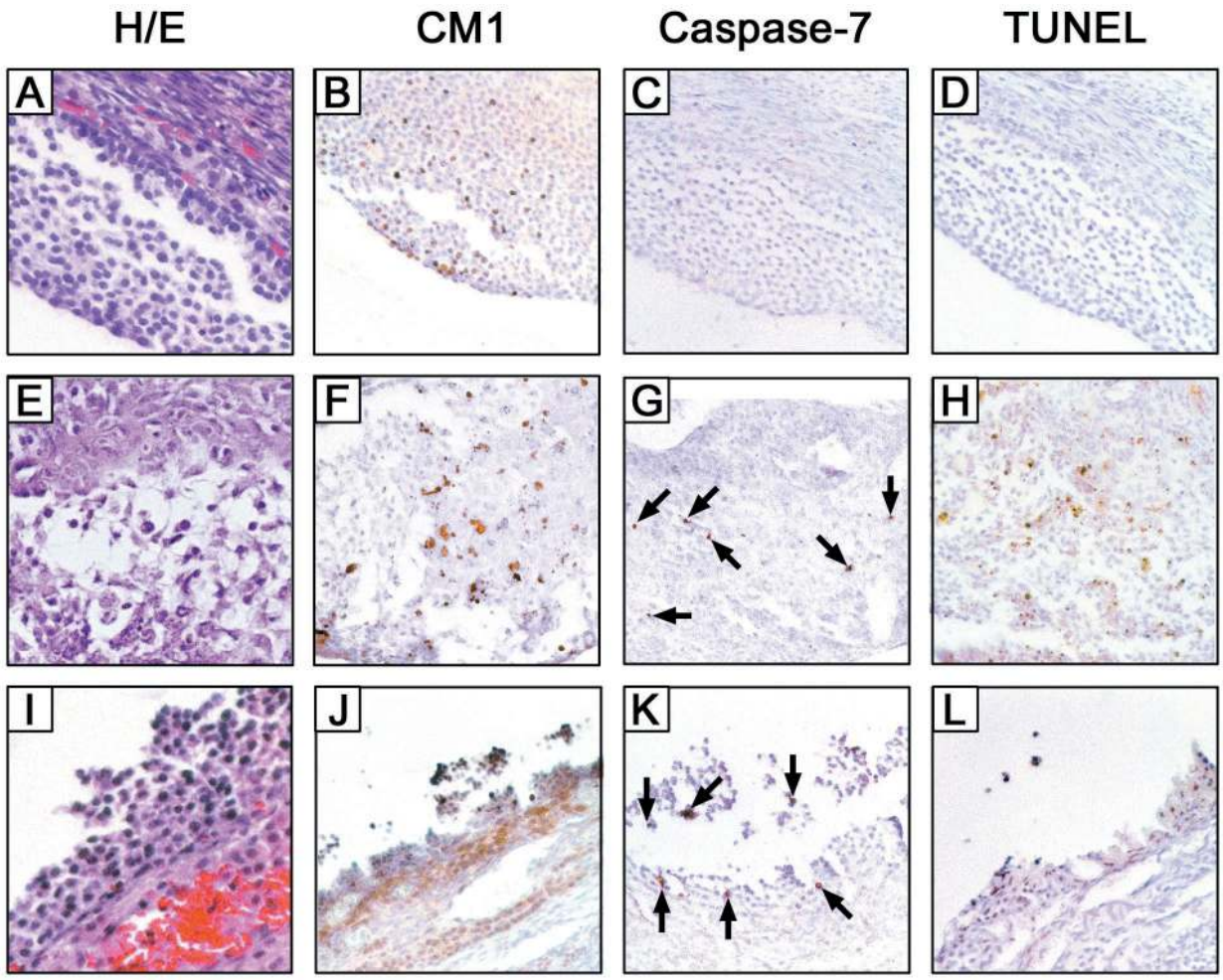

FIG. 10. Activation of caspase-3 and caspase-7 is correlated with granulosa cell apoptosis and antral follicle atresia in the human ovary. Time-related appearance of caspase-3 cleavage (CM1 immunoreactivity), caspase-7 cleavage, and *in situ* DNA fragmentation (TUNEL) in serial sections of antral follicles at very early (A–D), moderate (E–H), and advanced (I–L) stages of atresia *in vivo*. Processed caspase-7 (designated by *arrows* in G and K) is detected later than processed caspase-3, which is observed in many granulosa cells (B) before evidence of DNA cleavage *in situ* (D). The histological appearance of each follicle (after staining with hematoxylin and eosin, H/E) is also provided. Original magnifications, ×400. These data are representative of analysis of ovarian biopsies obtained from four different patients.

may be reflected by the greater number of oocytes ovulated in the *caspase-3*-null females, compared with their wild-type sisters, after treatment with exogenous gonadotropins. Although the basis of the 2-fold higher ovulatory response in the mutant mice remains to be established, the delay in atresia of maturing antral follicles in *caspase-3*-null females may allow for more follicles to be available for rescue from atresia by gonadotropins.

Although these data indicate that caspase-3 is functionally required for the normal execution of PCD in granulosa cells, the findings that granulosa cells lacking caspase-3 do eventually die suggest that caspase-independent mechanisms of cell death become activated (51) or that other caspase family members are involved. Regarding the latter, the low level of CM1 immunostaining observed in dying caspase-3-deficient granulosa cells provided one hint at the identity of at least one of these other family members. Previous work has shown that CM1, although highly selective for the cleaved form of caspase-3, exhibits a weak cross-reactivity to the large catalytic subunit of caspase-7 (43). These findings are not entirely unexpected, because 10 of the 13 amino acids in the cleaved caspase-3 peptide immunogen used to produce the CM1 antibody are conserved in caspase-7 (43). In addition, studies of hierarchical caspase activation after various apoptotic stimuli have shown that procaspase-7 is processed in parallel with procaspase-3 (36, 52, 53), and that caspase-3 is not needed for the activation of caspase-7 (52). Moreover, recent evidence indicates that a compensatory induction of caspase-7 activation occurs in caspase-3-deficient hepatocytes after exposure to a lethal stimulus (54).

Based on this information, we used a recently developed antibody that recognizes the cleaved form of caspase-7 to study its expression, in the absence or presence of functional caspase-3, in granulosa cells during apoptosis. Consistent with the idea that caspase-7 may compensate for the loss of caspase-3 function to eventually ensure granulosa cell death, we observed a positive correlation between the presence of cleaved caspase-7 and the occurrence of apoptosis. As this observation held true for both wild-type and *caspase-3* mutant granulosa cells, it may be that in wild-type cells

caspase-7 normally functions in tandem with caspase-3 during the execution phase of granulosa cell death. Similar results were obtained from a parallel analysis of caspases and apoptosis in granulosa cells of human ovarian follicles during atresia. This set of experiments revealed that intense CM1 immunoreactivity in granulosa cells appeared to herald their pending death, whereas cleaved caspase-7 was only detected in dying granulosa cells of moderately and grossly atretic antral follicles. Although these findings collectively support an evolutionarily conserved role for caspase-3 and caspase-7 in mediating granulosa cell death, a recent study has identified cleavage activation of procaspase-6, in addition to procaspase-3, in avian granulosa cells during apoptosis (55). Future analysis of ovaries in caspase-6-deficient female mice (16) should clarify whether this executioner caspase is involved in mammalian granulosa cell death.

In conclusion, this study has demonstrated the functional importance of caspase-3 in the execution of PCD in ovarian follicular somatic, but not germ, cells of the mouse ovary. We have also shown from studies of the human ovary that caspase-3 activation is probably an evolutionarily conserved feature of granulosa cell demise. In addition, we have provided evidence for the activation of caspase-7 in mouse and human granulosa cells during apoptosis, indicating that caspase-9 may serve to process at least two executioner caspases in somatic cells of the ovary during apoptosis. Interestingly, recent investigations have reported that caspase-3 is also activated in bovine (41, 56) and mouse (Rueda, B. R., and J. L. Tilly, unpublished observations) luteal cells during apoptosis. Such findings suggest that the requirement for caspase-3 in the normal execution of granulosa cell death shown herein may also be maintained as these cells transform into luteal cells after ovulation. Our current efforts are aimed at addressing this possibility as well as using a number of other gene knockout mouse lines to elucidate a molecular blueprint of how PCD is executed in oocytes, granulosa cells, and luteal cells via shared or cell lineage-specific signaling.

Acknowledgments

We thank Dr. Anu Srinivasan (IDUN Pharmaceuticals, Inc., La Jolla, CA) for generously providing the CM1 antibody, and we are indebted to Mr. Sam Riley (Massachusetts General Hospital) for outstanding technical assistance with the image analysis and data presentation.

References

1. **Morita Y, Tilly JL** 1999 Oocyte apoptosis: like sand through an hourglass. Dev Biol 213:1–17
2. **Tilly JL, Robles R** 1999 Apoptosis and its impact in clinical reproductive medicine. In: Fauser BCJM, Rutherford AJ, Strauss III JF, Van Steirteghem A (eds) Molecular Biology in Reproductive Medicine. Parthenon, New York, pp 79–101
3. **Baker TG** 1963 A quantitative and cytological study of germ cells in human ovaries. Proc R Soc Lond (B) 158:417–433
4. **Gougeon A** 1996 Regulation of ovarian follicular development in primates: facts and hypotheses. Endocr Rev 17:121–155
5. **Byskov AG** 1974 Cell kinetic studies of follicular atresia in the mouse ovary. J Reprod Fertil 37:277–285
6. **Kasuya K** 1997 Elimination of apoptotic granulosa cells by intact granulosa cells and macrophages in atretic mature follicles of the guinea pig ovary. Arch Histol Cytol 60:175–184
7. **Inoue S, Watanabe H, Saito H, Hiroi M, Tonosaki A** 2000 Elimination of atretic follicles from the mouse ovary: a TEM and immunohistochemical study. J Anat 196:103–110
8. **Green DR, Reed JC** 1998 Mitochondria and apoptosis. Science 281:1309–1312
9. **Budihardjo I, Oliver H, Lutter M, Luo X, Wang X** 1999 Biochemical pathways of caspase activation during apoptosis. Annu Rev Cell Dev Biol 15:269–290
10. **Reed JC** 1998 Bcl-2 family proteins. Oncogene 17:3225–3236
11. **Gross A, McDonnell JM, Korsmeyer SJ** 1999 BCL-2 family members and the mitochondria in apoptosis. Genes Dev 13:1899–1911
12. **Zou H, Henzel WJ, Liu X, Lutschg A, Wang X** 1997 Apaf-1, a human protein homologous to *C. elegans* CED-4, participates in cytochrome c-dependent activation of caspase-3. Cell 90:405–413
13. **Li P, Nijhawan D, Budihardjo I, Srinivasula SM, Ahmad M, Alnemri ES, Wang X** 1997 Cytochrome c and dATP-dependent formation of Apaf-1/caspase-9 complex initiates an apoptotic protease cascade. Cell 91:479–489
14. **Thornberry NA, Lazebnik Y** 1998 Caspases: enemies within. Science 281:1312–1316
15. **Cryns V, Yuan J** 1998 Proteases to die for. Genes Dev 12:1551–1570
16. **Zheng T, Hunot S, Kuida K, Flavell RA** 1999 Caspase knockouts: matters of life and death. Cell Death Differ 6:1043–1053
17. **Salvesen GS, Dixit VM** 1999 Caspase activation: the induced-proximity model. Proc Natl Acad Sci USA 96:10964–10967
18. **Tilly JL, Tilly KI, Kenton ML, Johnson AL** 1995 Expression of members of the *bcl-2* gene family in the immature rat ovary: equine chorionic gonadotropin-mediated inhibition of granulosa cell apoptosis is associated with decreased *bax* and constitutive *bcl-2* and *bcl-x_{long}* messenger RNA levels. Endocrinology 136:232–241
19. **Kugu K, Ratts VS, Piquette GN, Tilly KI, Tao X-J, Martimbeau S, Aberdeen GW, Krajewski S, Reed JC, Pepe GJ, Albrecht ED, Tilly JL** 1998 Analysis of apoptosis and expression of *bcl-2* gene family members in the human and baboon ovary. Cell Death Differ 5:67–76
20. **Jurisicova A, Latham K, Casper RF, Varmuza SL** 1998 Expression and regulation of genes associated with cell death during murine preimplantation embryo development. Mol Reprod Dev 51:243–253
21. **De Felici M, Di Carlo A, Pesce M, Iona S, Farrace MG, Piacentini M** 1999 Bcl-2 and Bax regulation of apoptosis in germ cells during prenatal oogenesis in the mouse embryo. Cell Death Differ 6:908–915
22. **Knudson CM, Tung KSK, Tourtellotte WG, Brown GAJ, Korsmeyer SJ** 1995 Bax-deficient mice with lymphoid hyperplasia and male germ cell death. Science 270:96–99
23. **Perez GI, Knudson CM, Leykin L, Korsmeyer SJ, Tilly JL** 1997 Apoptosis-associated signaling pathways are required for chemotherapy-mediated female germ cell destruction. Nat Med 3:1228–1332
24. **Perez GI, Robles R, Knudson CM, Flaws JA, Korsmeyer SJ, Tilly JL** 1999 Prolongation of ovarian lifespan into advanced chronological age by *Bax*-deficiency. Nat Genet 21:200–203
25. **Perez GI, Trbovich AM, Gosden RG, Tilly JL** 2000 Mitochondria and the death of oocytes. Nature 403:500–501
26. **Robles R, Tao X-J, Trbovich AM, Maravei DV, Nahum R, Perez GI, Tilly KI, Tilly JL** 1999 Localization, regulation and possible consequences of apoptotic protease-activating factor-1 (Apaf-1) expression in granulosa cells of the mouse ovary. Endocrinology 140:2641–2644
27. **Flaws JA, Kugu K, Trbovich AM, DeSanti A, Tilly KI, Hirshfield AN, Tilly JL** 1995 Interleukin-1β-converting enzyme-related proteases (IRPs) and mammalian cell death: dissociation of IRP-induced oligonucleosomal endonuclease activity from morphological apoptosis in granulosa cells of the ovarian follicle. Endocrinology 136:5042–5053
28. **Boone DL, Tsang BK** 1998 Caspase-3 in the rat ovary: localization and possible role in follicular atresia and luteal regression. Biol Reprod 58:1533–1539
29. **Jänicke RU, Ng P, Sprengart ML, Porter AG** 1998 Caspase-3 is required for α-fodrin cleavage but dispensable for cleavage of other death substrates in apoptosis. J Biol Chem 273:15540–15545
30. **Maravei DV, Trbovich AM, Perez GI, Tilly KI, Talanian RV, Banach D, Wong WW, Tilly JL** 1997 Cleavage of cytoskeletal proteins by caspases during ovarian cell death: evidence that cell-free systems do not always mimic apoptotic events in intact cells. Cell Death Differ 4:707–712
31. **Thornberry NA, Rano TA, Peterson EP, Rasper DM, Timkey T, Garcia-Calvo M, Houtzager VM, Nordstrom PA, Roy S, Vaillancourt JP, Chapman KT, Nicholson DW** 1997 A combinatorial approach defines specificities of members of the caspase family and granzyme B. Functional relationships established for key mediators of apoptosis. J Biol Chem 272:17907–17911
32. **Maravei DV, Morita Y, Kuida K, Tilly JL** 1999 Pre- and postnatal ovarian apoptosis defects in caspase-9-deficient mice. Mol Biol Cell [Suppl] 10:352a
33. **Exley GE, Tang C, McElhinny AS, Warner CM** 1999 Expression of caspase and BCL-2 apoptotic family members in mouse preimplantation embryos. Biol Reprod 61:231–239
34. **Bergeron L, Perez GI, Mcdonald G, Shi L, Sun Y, Jurisicova A, Varmuza S, Latham KE, Flaws JA, Salter J, Hara H, Moskowitz MA, Li E, Greenberg AH, Tilly JL, Yuan J** 1998 Defects in regulation of apoptosis in caspase-2-deficient mice. Genes Dev 12:1304–1314
35. **Perez GI, Tao X-J, Tilly JL** 1999 Fragmentation and death (*a.k.a.* apoptosis) of ovulated oocytes. Mol Hum Reprod 5:414–420
36. **Kuida K, Zheng TS, Na S, Kuan C, Yang D, Karasuyama H, Rakic P, Flavell RA** 1996 Decreased apoptosis in the brain and premature lethality in CPP32-deficient mice. Nature 384:368–372
37. **Morita Y, Perez GI, Maravei DV, Tilly KI, Tilly JL** 1999 Targeted expression

of Bcl-2 in mouse oocytes inhibits ovarian follicle atresia and prevents spontaneous and chemotherapy-induced oocyte apoptosis *in vitro*. Mol Endocrinol 13:841–850

38. **Morita Y, Perez GI, Paris F, Miranda S, Ehleiter D, Haimovitz-Friedman A, Fuks Z, Xie Z, Reed JC, Schuchman EH, Kolesnick RN, Tilly JL** 2000 Oocyte apoptosis is suppressed by disruption of the *acid sphingomyelinase* gene or by sphingosine-1-phosphate therapy. Nat Med 6:1109–1114
39. **Tilly JL, Hsueh AJW** 1993 Microscale autoradiographic method for the qualitative and quantitative analysis of apoptotic DNA fragmentation. J Cell Physiol 154:519–526
40. **Tilly JL** 1994 Use of the terminal transferase DNA labeling reaction for the biochemical and *in situ* analysis of apoptosis. In: Celis JE (ed) Cell Biology: A Laboratory Handbook. Academic Press, San Diego, vol 1:330–337
41. **Rueda BR, Hendry IR, Ndjountche L, Suter J, Davis JS** 2000 Stress-induced mitogen-activated protein kinase signaling in the corpus luteum. Mol Cell Endocrinol 164:59–67
42. **Shi SR, Key ME, Kalra KL** 1991 Antigen retrieval in formalin-fixed, paraffin-embedded tissues: an enhancement method for immunohistochemical staining based on microwave oven heating of tissue sections. J Histochem Cytochem 39:741–748
43. **Srinivasan A, Roth KA, Sayers RO, Shindler KS, Wong AM, Fritz LC, Tomaselli KJ** 1998 *In situ* detection of activated caspase-3 in apoptotic neurons in the developing nervous system. Cell Death Differ 5:1004–1016
44. **Hughes Jr FM, Gorospe WC** 1991 Biochemical identification of apoptosis (programmed cell death) in granulosa cells: evidence for a potential mechanism underlying follicular atresia. Endocrinology 129:2415–2422
45. **Tilly JL, Billig H, Kowalski KI, Hsueh AJW** 1992 Epidermal growth factor and basic fibroblast growth factor suppress the spontaneous onset of apoptosis in cultured rat ovarian granulosa cells and follicles by a tyrosine kinase-dependent mechanism. Mol Endocrinol 6:1942–1950
46. **Flaws JA, DeSanti A, Tilly KI, Javid RO, Kugu K, Johnson AL, Hirshfield AN, Tilly JL** 1995 Vasoactive intestinal peptide-mediated suppression of apoptosis in the ovary: potential mechanisms of action and evidence of a conserved anti-atretogenic role through evolution. Endocrinology 136:4351–4359
47. **Garcia-Calvo M, Peterson EP, Rasper DM, Vaillancourt JP, Zamboni R, Nicholson DW, Thornberry NA** 1999 Purification and catalytic properties of human caspase family members. Cell Death Differ 6:362–369
48. **Zhang Y, Goodyer C, LeBlanc A** 2000 Selective and protracted apoptosis in human primary neurons microinjected with active caspase-3, -6, -7, and -8. J Neurosci 20:8384–8389
49. **Enari M, Sakahira H, Yokoyama H, Okawa K, Iwamatsu A, Nagata S** 1998 A caspase-activated DNase that degrades DNA during apoptosis, and its inhibitor ICAD. Nature 391:43–50
50. **Zheng TS, Schlosser SF, Dao T, Hingorani R, Crispe IN, Boyer JL, Flavell RA** 1998 Caspase-3 controls both cytoplasmic and nuclear events associated with Fas-mediated apoptosis *in vivo*. Proc Natl Acad Sci USA 95:13618–13623
51. **Susin SA, Daugas E, Ravagnan L, Samejima K, Zamzami N, Loeffler M, Costantini P, Ferri KF, Irinopoulou T, Prévost M-C, Brothers G, Mak TW, Penninger J, Earnshaw WC, Kroemer G** 2000 Two distinct pathways leading to nuclear apoptosis. J Exp Med 192:571–579
52. **Slee EA, Harte MT, Kluck RM, Wolf BB, Casiano CA, Newmeyer DD, Wang H-G, Reed JC, Nicholson DW, Alnemri ES, Green DR, Martin SJ** 1999 Ordering the cytochrome c-initiated caspase cascade: hierarchical activation of caspases-2, -3, -6, -7, -8, and -10 in a caspase-9-dependent manner. J Cell Biol 144:281–292
53. **Sun X-M, MacFarlane M, Zhuang J, Wolf BB, Green DR, Cohen GM** 1999 Distinct caspase cascades are initiated in receptor-mediated and chemical-induced apoptosis. J Biol Chem 274:5053–5060
54. **Zheng TS, Hunot S, Kuida K, Momo T, Srinivasan A, Nicholson DW, Lazebnik Y, Flavell RA** 2000 Deficiency in caspase-9 or caspase-3 induces compensatory caspase activation. Nat Med 6:1241–1247
55. **Johnson AL, Bridgham JT** 2000 Caspase-3 and -6 expression and enzyme activity in hen granulosa cells. Biol Reprod 62:589–598
56. **Rueda BR, Hendry IR, Tilly JL, Hamernik DL** 1999 Accumulation of *caspase*-3 mRNA and induction of caspase activity in the ovine corpus luteum following prostaglandin-$F_{2\alpha}$ treatment *in vivo*. Biol Reprod 60:1087–1092